Tests of concrete-filled double skin CHS composite stub columns

Xiao-Ling Zhao†, Raphael Grzebieta‡ and Mohamed Elchalakani‡†

Department of Civil Engineering, Monash University, Victoria 3800, Australia

(Received October 8, Accepted March 5, 2002)

Abstract.   This paper describes a series of compression tests carried out on concrete filled double skin tubes (CFDST). Both outer and inner tubes are cold-formed circular hollow sections (CHS). Six section sizes were chosen for the outer tubes with diameter-to-thickness ratio ranging from 19 to 57. Two section sizes are chosen for the inner tubes with diameter-to-thickness ratio of 17 and 33. The failure modes, strength, ductility and energy absorption of CFDST are compared with those of empty single skin tubes. Increased ductility and energy absorption have been observed for CFDST especially for those having slender outer tubes with larger diameter-to-thickness ratio. Predictions from several theoretical models are compared with the ultimate strength of CFDST stub columns obtained in the tests. The proposed formula was found to be in good agreement with the experimental data.

Keywords: concrete-filled tubes; double-skin composite sections; circular hollow sections.

1. Introduction

The concept of "double skin" composite construction was originally devised for use in submerged tube tunnels (Tomlinson *et al.* (1989)). It is believed that it also has a potential in nuclear containment, liquid and gas retaining structures and blast resistant shelters (Wright *et al.* 1991a, 1991b). Concrete filled double skin tubes (CFDST) consist of two concentric steel cylinders or shells with the annulus between them filled with concrete (see Fig. 1). This form of construction can be applied to sea-bed vessels, in the legs of offshore platforms in deep water, to large diameter columns and to structures subjected to ice loading (Montague 1978, Shakir-Khalil 1991, Wei *et al.* 1995, Lin and Tsai 2001). Recently CFDST have been used as high-rise bridge piers in Japan (Sugimoto *et al.* 1997, Yagishita *et al.* 2000) to reduce the structure weight while still maintaining a large energy absorption capacity against earthquake loading.

A research project on "Tubular Structures under High Amplitude Dynamic Loading" is currently underway at Monash University, Australia. Some results on void-filled tubes subjected to bending and compression tests were reported elsewhere (Zhao and Grzebieta 1999, Zhao *et al.* 1999, Zhao *et al.* 2002, Elchalakani *et al.* 2002a, b). Part of the project is to study the behaviour of CFDST. Square Hollow Sections (SHS) or Circular Hollow Sections (CHS) can be used as inner tubes or outer tubes, leading to several

---

†Professor
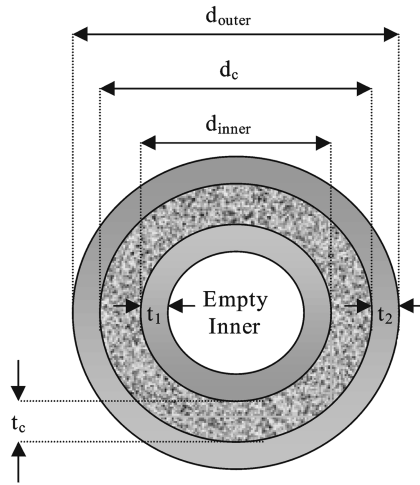‡Associate Professor
‡†Structural Eng. Post gad.

Fig. 1 Concrete filled double skin tubes (CFDST)-both inner and outer tubes are CHS

combinations. This paper only addresses the case where both inner and outer tubes are CHS (see Fig. 1), whereas other cases are reported elsewhere (Zhao and Grzebieta 2002, Elchalakani *et al.* 2002c).

This paper describes a series of compression tests carried out on concrete filled double skin CHS tubes. Both outer and inner tubes are cold-formed circular hollow sections (CHS). Six section sizes were chosen for the outer tubes with diameter-to-thickness ratio ranging from 19 to 57. Two section sizes are chosen for the inner tubes with diameter-to-thickness ratio of 17 and 33. Some sections are fully effective (i.e. full section yielding can be achieved in compression) while some sections are not fully effective (i.e. full section yield cannot be achieved in compression due to the local buckling) in order to investigate the effect of *D/t* ratio on the behaviour of double skin composite stub columns. The failure modes of the outer and inner tubes are studied in detail. It has been observed that the ductility and energy absorption increases significantly for CFDST especially for those having slender outer tubes. The predicted ultimate strength of CFDST stub columns using AISC-LRFD (1999), ACI (1995), EC4 (1992) and Kato model (1996) is compared with experimental data. A simple formula is proposed in this paper to predict the ultimate strength of CFDST stub columns.

2. Material properties

The circular hollow secitons were supplied by BHP Structural Pipeline and Products (now OneSteel). They are manufactured using a cold forming process in accordance with the Australian Standard AS1163 (SAA 1991a). The nominal yield stress of these CHS was 350 MPa. The average values of measured dimensions and material properties for the CHS used in this project are summarised in Table 1, where a cross-section ID number (C1 to C8) is given. Tensile coupon tests were performed according to AS1391 (SAA (1991b). The 0.2% proof stress was adopted as the yield stress. The compressive strength of the concrete was determined using concrete cylinders with a diameter of 100 mm and a height of 200 mm (see Fig. 2). The concrete cylinders were cured for 28 days and the average compressive strength (f_c) was 63.4 MPa.

Table 1 Measured dimensions and material properties

Tube	Section ID	d_m (mm)	t_m (mm)	d_m/t_m	$\lambda_e = (d_m/t_m)(\sigma_y/250)$	σ_y (MPa)
Outer tube	C1	114.5	5.9	19.41	35.24	454
	C2	114.6	4.7	24.38	40.57	416
	C3	114.4	3.5	32.69	59.23	453
	C4	114.2	3.0	38.07	65.47	430
	C5	165.1	3.5	47.17	80.19	433
	C6	165.3	2.9	57.00	90.06	395
Inner tube	C7	48.4	2.8	17.29	29.39	425
	C8	101.8	3.1	32.84	53.86	410

Fig. 2 Concrete cylinders

3. Test specimens and test procedures

Three stub column tests on empty CHS (C4, C7 and C8) were performed in a 500 kN capacity Baldwin testing machine. Five specimens (C1, C2, C3, C5 and C6) were tested in a 5000 kN Amsler universal testing machine. The specimens were labelled C1 to C8 for empty CHS stub columns. The length of the specimen was determined according to AS/NZS4600 (SAA 1996). The length of C7 was 150 mm whereas the length of C1 to C8 was 400 mm. The test set up of empty CHS stub columns is shown in Fig. 3(a). Six stub column tests on CFDST were performed in a 5000 kN capacity Amsler machine. The specimens were labelled as shown in Table 2 where the dimensions defined in Fig. 1 are given. The length of the CFDST specimens was 400 mm. The ends of all stub columns were milled flat before testing so that they could be properly seated on the rigid end platen's of the testing machine. Shortening of the column was measured by using two Linear Variable Displacement Transducers placed between the two parallel end platens and measuring each platenís movement relative to the other. The test set up of CFDST stub columns is shown in Fig. 3(b). A displacement control was used with a rate of 0.5 mm/minute.

Fig. 3 Test set up (a) empty CHS stub columns in baldwin testing machine, (b) CFDST stub columns in amsler testing machine

Table 2 Dimensions of CFDST stub columns

Specimen label	d_{outer} (mm)	d_{inner} (mm)	d_c (mm)	t_1 (mm)	t_2 (mm)	t_c (mm)	$A_{outerCHS}$ (mm^2)	$A_{innerCHS}$ (mm^2)	A_c (mm^2)
C1C7	114.5	48.4	102.7	2.8	5.9	27.2	2013	401	6444
C2C7	114.6	48.4	105.2	2.8	4.7	28.4	1623	401	6852
C3C7	114.4	48.4	107.4	2.8	3.5	29.5	1219	401	7220
C4C7	114.2	48.4	108.2	2.8	3.0	29.9	1048	401	7355
C5C8	165.1	101.8	158.1	3.1	3.5	28.2	1777	961	11492
C6C8	165.3	101.8	159.5	3.1	2.9	28.9	1480	961	11841

4. Test results

4.1. Empty CHS

The failure mode of empty CHS is shown in Fig. 4. It can be seen that an "elephant foot" mechanism formed for all empty CHS stub columns. This failure mode is expected for CHS with small *D/t* ratios (Grzebieta 1990). The load versus axial deflection curves are presented in Fig. 5. The ultimate load capacity (P_u) achieved in the test is listed in Table 3. The full section yield capacity (P_{yt}), which is calculated as a product of the measured cross-section area and measured yield stress, is listed in Column 3 of Table 3. The full section yield capacity (P_{yn}) based on the nominal yield stress is also listed in Column 4 of Table 3. The ratios (P_u / P_{yt} and P_u / P_{yn}) are given in Table 3 as well as plotted in Fig. 6 against the section slenderness. The yield slenderness limit was $\lambda_{ey} = 82$, below which a section can achieve full yielding, as specified in the Australian/New Zealand Standard for Steel Structures AS/NZS4100 (SAA 1998). It is also plotted in Fig. 6. It seems that the yield slenderness limit specified in AS/NZS4100 is satisfactory for cold-formed CHS stub columns.
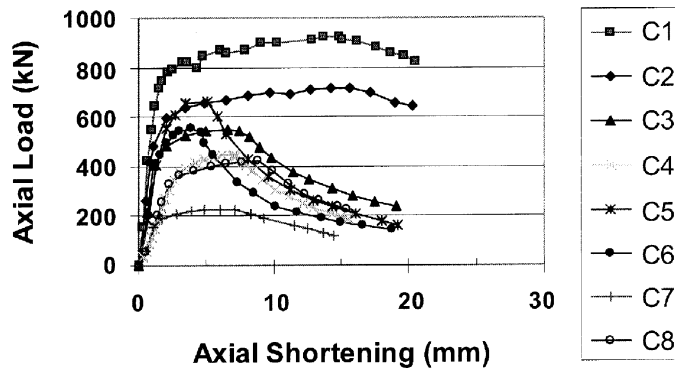
Fig. 4 Failure modes of empty CHS stub columns

Fig. 5 Load versus axial deflection curves for empty CHS stub columns

4.2. CFDST

The failure modes of outer tubes are shown in Fig. 7. It can be seen that the outer tube behaves the same way (i.e. forming an outward folding mechanism) as a concrete filled tube. Two typical failure modes were observed, one is the "elephant foot mode" formed near the end and the other is an outward folding mechanism formed along the diagonal direction (called "diagonal shear mode" in this paper) as shown in Fig. 8. Similar modes of failure were observed in Elchalakani *et al.* (2002c) and Shakir-Khalil (1991). A view of the CFDST after opening is shown in Fig. 8(b). The failure of the inner tube may be described as "distorted diamond" mode shown in Fig. 9. Undistorted diamond mode often forms for CHS with diameter-to-thickness ratio larger than 60 subjected to uniform axial compression (Grzebieta (1990). It can be seen that the inner tube behaves differently compared with empty CHS stub columns that normally form "elephant foot" at one end as shown in Fig. 4. The development of failure modes for CFDST (e.g. C4C7 and C5C8) is illustrated in Appendix A. It can be seen that the "elephant foot" forms first (see Fig. A.1(d) and Fig. A.2(e)) followed by the "diagonal shear" mode

Table 3 Test results of empty CHS stub columns

Specimen label	P_u (kN)	P_{yt} (kN)	P_{yn} (kN)	P_u/P_{yt}	P_u/P_{yn}	Energy W_{CHS} (kNm)
C1	927	914	705	1.014	1.316	12.5
C2	719	675	568	1.065	1.266	9.5
C3	560	552	427	1.014	1.312	6.0
C4	454	451	367	1.007	1.238	4.6
C5	674	755	622	0.893	1.084	6.5
C6	553	584	518	0.946	1.068	4.8
C7	228	170	140	1.337	1.624	2.5
C8	414	394	336	1.050	1.231	4.5
Mean	–			1.041	1.267	–
Coefficient of variation				0.127	0.136	
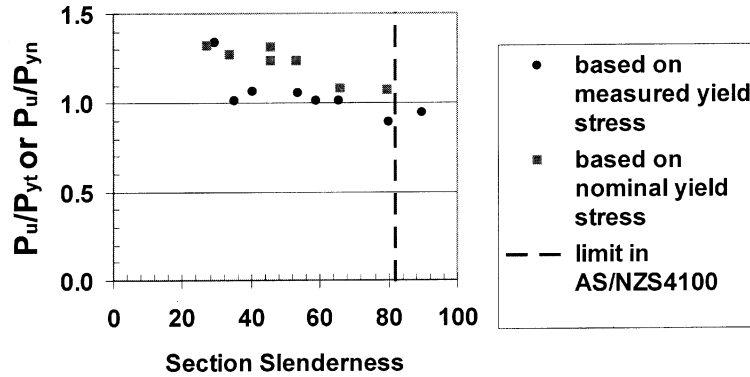
Fig. 6 Section slenderness (λ_e) versus P_u/P_{yt} and P_u/P_{yn}

(see Fig. A.1(f) and Fig. A.2(g)). The axial load versus axial shortening curves are given in Fig. 10 for CFDST specimens. The maximum test load (P_{test}) for each specimen is listed in Column 2 of Table 4.

5. Strength prediction

5.1. Existing codes

The design equations for composite columns in the following codes are applied to CFDST in this section, with some modifications made when required.

5.1.1. CFDST Strength to EC4 (1992)
In EC4 (1992), the cross sectional axial strength of composite stub columns includes the enhancement of the concrete axial compressive strength due to confinement and the corresponding

Fig. 7 CFDST specimens after testing

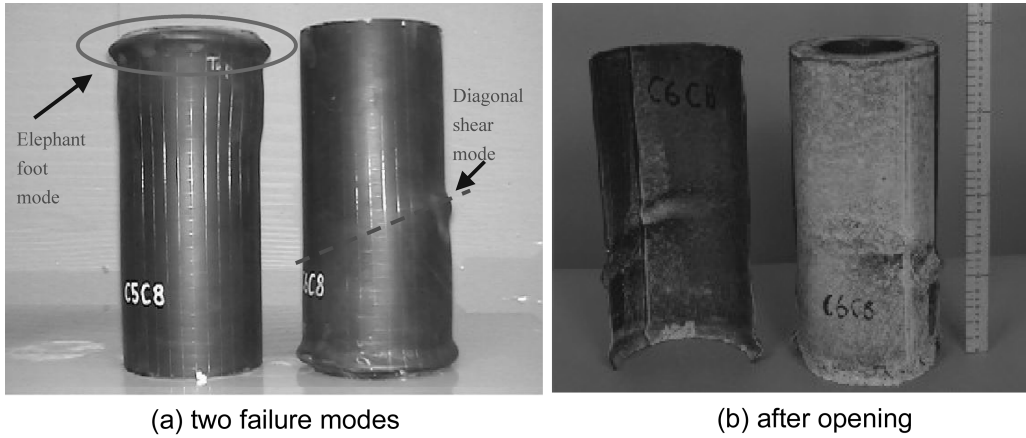(a) two failure modes

(b) after opening

Fig. 8 Typical failure modes of CFDST

reduction in steel axial compressive strength due to the circumferential tension in the steel tube resulting from the confinement of the concrete. The nominal strength is expressed as

$$P_{EC4} = (A_s f_y)(\eta_2 / \gamma_s) + A_c[1 + \eta_1(t/D)(f_{ys}/f_c)](f_c / \gamma_c)$$ (1)

The enhancement of concrete strength can be taken into account only when the column is short ($\bar{\lambda} < 0.5$). The coefficients η_1 and η_2 for concentrically loaded columns are given by

$$\eta_1 = 4.9 - 18.5\bar{\lambda} + 17\bar{\lambda}^2 \geq 0.0$$

$$\eta_2 = 0.25(3 + 2\bar{\lambda}) \leq 1.0$$

$$\bar{\lambda} = \sqrt{\frac{(A_s f_y) + 0.85 A_c f_c}{P_e}}$$

(a) After opening

(b) Top view
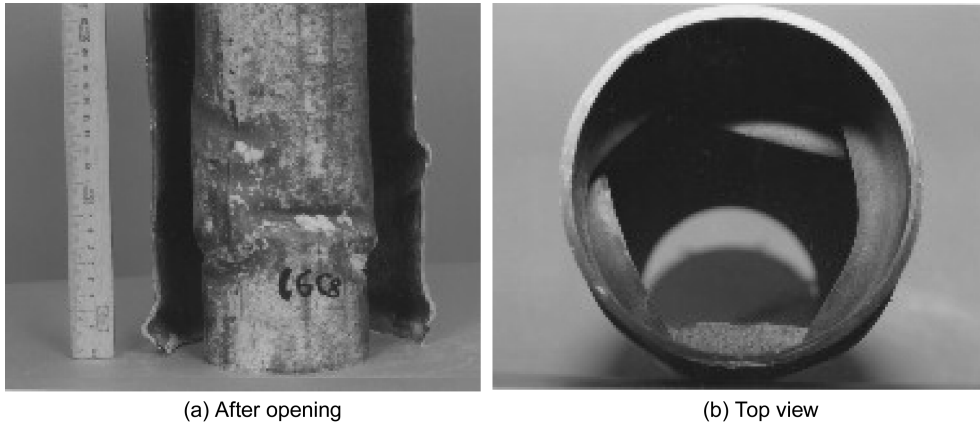
Fig. 9 Failure modes of the inner CHS in CFDST
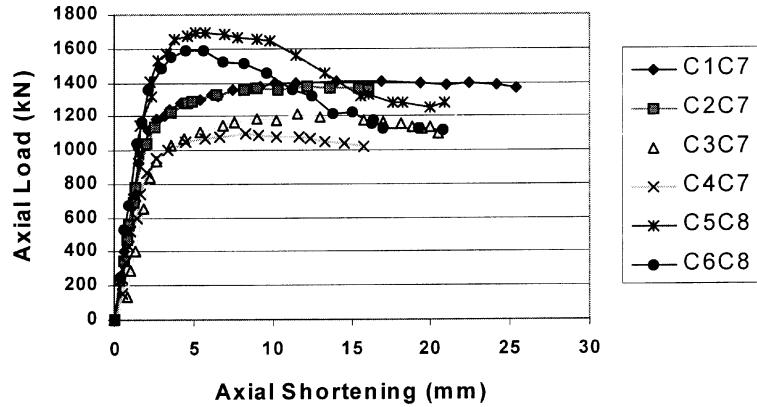
Fig. 10 Axial load versus axial shortening curves

Table 4 Test results of CFDST stub columns (Strength)

Specimen label (1)	P_{test} (kN) (2)	P_{EC4} (kN) (3)	P_{AISC} (kN) (4)	P_{ACI} (kN) (5)	P_{Kato} (kN) (6)	P_{theory} (kN) (7)	P_{EC4}/P_{test} (8)	P_{AISC}/P_{test} (9)	P_{ACI}/P_{test} (10)	P_{Kato}/P_{test} (11)	P_{theory}/P_{test} (12)
C1C7	1415	1729	1422	1217	1534	1432	1.222	1.005	0.860	1.084	1.012
C2C7	1380	1466	1207	1033	1323	1215	1.062	0.874	0.748	0.959	0.880
C3C7	1210	1336	1104	945	1226	1112	1.104	0.912	0.781	1.014	0.919
C4C7	1110	1213	1010	865	1134	1017	1.093	0.910	0.779	1.022	0.917
C5C8	1705	2024	1777	1515	1965	1783	1.187	1.042	0.889	1.152	1.046
C6C8	1605	1817	1611	1374	1804	1617	1.132	1.004	0.856	1.124	1.007
Mean							1.133	0.958	0.819	1.059	0.963
Coefficient of variation							0.0533	0.0704	0.0690	0.0695	0.0690

$$P_e = \frac{(EI)_e \pi^2}{(kL)^2}$$

$$(EI)_e = E_s I_s + 0.8 E_c I_c$$

For CFDST stub columns in this paper:

$A_s f_y = A_{outerCHS} \cdot f_{y,outerCHS} + A_{innerCHS} \cdot f_{y,innerCHS}$ where $A_{outerCHS}$ is the area of the outer CHS and $A_{innerCHS}$ is the area of the inner CHS given in Table 2, $f_{y,outerCHS}$ is the yield stress of the outer CHS (C1 to C6) and $f_{y,innerCHS}$ is the yield stress of the inner CHS (C7 and C8) given in Table 1.

A_c = area of concrete given in Table 2.

f_c = compressive strength of concrete

f_{ys} = yield stress of the outer SHS = $f_{y,outerCHS}$

t = thickness of the outer CHS = t_2 in Fig. 1

D = diameter of the outer CHS = d_{outer} in Fig. 1

γ_c = partial safety factor for the concrete taken as 1.0

γ_s = partial safety factor for the structural steel taken as 1.0

kL = effective length of column where k = 0.7 for fixed end and L is the length of CFDST specimens

E_s = modulus of elasticity of steel

E_c = modulus of elasticity of concrete taken as $0.043 \cdot \rho^{1.5} \cdot \sqrt{f_c}$ where ρ is the density of the concrete (=2400 kg/m^3) as given in AS3600 (SAA, 1994)

$I_s = I_{outerCHS} + I_{innerCHS}$ where $I_{outerCHS}$ is the second moment of area for the outer CHS and $I_{innerCHS}$ is the moment of area for the inner CHS

I_c = second moment of area for the concrete

The predicted strength using EC4 (1992) is listed in Column 3 of Table 4. It is compared with the experimental values in Column 8 of Table 4. It seems that Eq. (1) slightly overestimates the strength of CFDST stub columns.

5.1.2. CFDST Strength to AISC-LRFD (1999)

The nominal strength for composite compression members are given as:

$$P_{AISC} = A_s \cdot F_{cr} \tag{2}$$

$$F_{cr} = (0.658^{\lambda_c^2}) f_{my} \qquad \text{For } \lambda_c \leq 1.5$$

$$F_{cr} = \left(\frac{0.877}{\lambda_c^2}\right) f_{my} \qquad \text{For } \lambda_c > 1.5$$

$$\lambda_c = \frac{kL}{r\pi} \sqrt{\frac{f_{my}}{E_m}}$$

The idea behind this method of design is to substitute the section properties of the composite column to an equivalent steel section with modified properties of f_{my} and E_m:

$$f_{my} = f_y + c_2 f_c (A_c / A_s)$$

$$E_m = E_s + c_3 E_c (A_c / A_s)$$

For CFDST stub columns in this paper:
A_c, f_c, kL, E_c and E_s are defined in Section 5.1.1 of this paper.

$A_s = A_{outerCHS} + A_{innerCHS}$ where $A_{outerCHS}$ is the area of the outer CHS and $A_{innerCHS}$ is the area of the inner CHS given in Table 2.

f_y = average yield stress of the outer and inner CHS = $\dfrac{f_{y,outerCHS} \cdot A_{outerCHS} + f_{y,innerCHS} \cdot A_{innerCHS}}{A_{outerCHS} + A_{innerCHS}}$

where $f_{y,outerCHS}$ is the yield stress of the outer CHS (C1 to C6) and $f_{y,innerCHS}$ is the yield stress of the inner CHS (C7 and C8) given in Table 1.

$c_2 = 0.85$
$c_3 = 0.4$
r = combined radius of gyration = $\sqrt{\dfrac{I_{outerCHS} + I_{innerCHS}}{A_{outerCHS} + A_{innerCHS}}}$ where $I_{outerCHS}$ is the second moment of area for the outer CHS and $I_{innerCHS}$ is the moment of area for the inner CHS.

The predicted strength using AISC-LRFD (1999) is listed in Column 4 of Table 4. It is compared with the experimental values in Column 9 of Table 4 where a mean value of 0.958 is obtained for P_{AISC}/P_{test}.

5.1.3. CFDST Strength to ACI 318-95
The nominal axial strength of composite column is given by

$$P_{ACI} = 0.85 \cdot [0.85 f_c A_c + (f_y A_s)] \tag{3}$$

For CFDST stub columns in this paper:
A_c, f_c and $(f_y A_s)$ are defined in Section 5.1.1 of this paper. The predicted strength using ACI 318 (1995) is listed in Column 5 of Table 4. It is compared with the experimental values in Column 10 of Table 4. It seems that Eq. (3) underestimates the strength of CFDST stub columns. This may be due to the reduction factor of 0.85 (located outside the parenthesis) used in Eq. (3).

5.1.4. CFDST Strength to Kato (1996)
Kato (1996) extended the ISO standards for steel structures for the use in the design of composite columns. Curve "b" was selected to allow for imperfections found in the steel tube. The enhancement due to confinement of the concrete was considered. No reduction was allowed for the steel axial compressive strength. The nominal strength of a composite section is expressed as

$$P_{Kato} = g P_y \tag{4}$$
$$P_y = (A_s f_y) + \beta A_c f_c$$

$\beta = 1.1$ for concrete-filled circular tubes

$$g = B(1 - \sqrt{1 - C})$$

$$B = \frac{1 + 0.34(\bar{\lambda} - 0.2) + \bar{\lambda}^2}{2\bar{\lambda}^2}$$

$$C = (B\bar{\lambda})^{-2}$$

$$\bar{\lambda} = \frac{kL}{\pi} \sqrt{\frac{A_s f_y + \beta A_c f_c}{E_s I_s + E_c I_c}}$$

<u>For CFDST stub columns in this paper:</u>

All the symbols are defined in Section 5.1.1 of this paper. The predicted strength using Kato (1996) is listed in Table 4 (column 6) where the enhancement factor β of 1.1 was used as specified in the code for concrete filled circular tubes. It is compared with the experimental values in Column 11 in Table 4 where a mean value of 1.059 was obtained for P_{Kato}/P_{test}. It can be shown that the mean ratio becomes 1.021 if the enhancement factor β of 1.0 was used.

5.2. Proposed formula

The ultimate strength (P_{theory}) of CFDST is estimated in this paper using the sum of the section capacities of the concrete, the outer steel tube and the inner steel tube, i.e.

$$P_{theory} = P_{concrete} + P_{outer} + P_{inner} \tag{5}$$

in which,

$$P_{concrete} = f_c \cdot A_c = f_c \cdot \frac{\pi}{4}(d_c^2 - d_{inner}^2) \tag{6}$$

$$P_{outer} = \sigma_y \cdot A_{outerCHS} = \sigma_y \cdot \frac{\pi}{4} \cdot (d_{outer}^2 - d_c^2) \tag{7}$$

$$P_{inner} = \sigma_y \cdot A_{innerCHS} = \sigma_y \cdot \frac{\pi}{4} \cdot [d_{inner}^2 - (d_{inner} - 2 \cdot t_1)^2] \tag{8}$$

where σ_y is the yield stress given in Table 1, the dimensions (d_{outer}, d_{inner}, d_c, t_1) in Eqs. (6), (7) and (8) are defined in Fig. 1 and Table 2.

The predicted ultimate strength (P_{theory}) is compared in Table 4 (column 12) with the experimental data (P_{test}). A good agreement was obtained with a mean value of 0.963 and a coefficient of variation of 0.069 for P_{theory}/P_{test}.

6. Ductility and energy ratio

The axial load versus axial shortening curve for specimen C1C7 is compared in Fig. 11(a) with that of the empty outer tube C1 with d_{outer}/t_2 of 17.4. Similar comparison is made in Fig. 11(b) for specimen C4C7 which has an outer tube C4 with a much larger d_{outer}/t_2 ratio of 38.0. It can be seen that the double-skin filling increases the ductility of CFDST specimens especially for slender outer tubes where the CFDST maintained higher loads for very large deformation compared to hollow outer sections. Comparisons are shown in Table 5 and Fig. 12 for energy absorption calculated using the area under the load-deflection curve when axial shortening is up to 15 mm. It can be seen that there is a significant increase in energy absorption especially for more slender sections, which emphasizes the efficiency of void filling of thin CHS. The trend can be seen for specimens with the same inner tube, i.e. C7 (compare C1C7, C2C7, C3C7 and C4C7) or C8 (compare C5C8 and C6C8). The trend is valid when comparison is made between CFDST and the outer CHS in Fig. 12(a), as well as between CFDST and the outer plus inner tubes in Fig. 12(b).
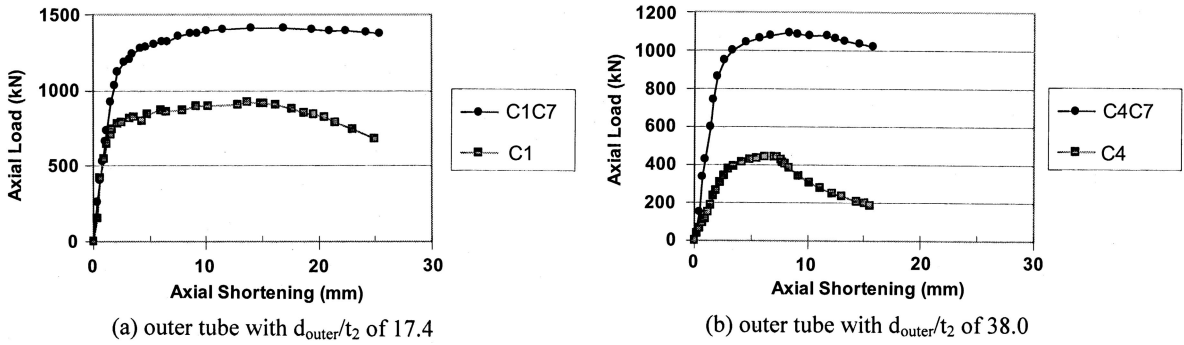
(a) outer tube with d_{outer}/t_2 of 17.4　　　　　(b) outer tube with d_{outer}/t_2 of 38.0

Fig. 11 Comparison between CFDST and empty tubes

Table 5 Test results of CFDST stub columns (Energy)

Specimen label	Outer CHS section slenderness	W_{CFDST} (kNm)	$W_{CHS+CHS}$	W_{CFDST}/W_{CHS}	$W_{CFDST}/W_{CHS+CHS}$
C1C7	35.24	19.9	15.0	1.59	1.32
C2C7	40.57	17.6	12.0	1.86	1.47
C3C7	59.23	14.8	8.5	2.47	1.74
C4C7	65.47	14.6	7.1	3.18	2.06
C5C8	71.51	11.5	11.0	1.76	1.04
C6C8	81.40	20.9	9.3	4.40	2.26

7. Conclusions

The following conclusions and observations are made based on the limited tests described in this paper, where the diameter-to-thickness ratio ranged from 19 to 57 for the outer CHS, and from 17 to 33 for the inner CHS.

- The failure mode of empty CHS was the "elephant foot" mechanism.
- Two typical failure modes were observed for CFDST, one is the "elephant foot mode" formed near the end and the other is an outward folding mechanism formed along the diagonal direction (called "diagonal shear mode" in this paper). It was found that "elephant foot" forms first followed by the "diagonal shear" mode.
- The inner tube in CFDST stub columns behaves differently compared with empty CHS ones that normally form "elephant foot" at one end.
- The yield slenderness limit of λ_{ey}=82 specified in the Australian Standard for Steel Structures AS4100 [SAA 1998] is satisfactory for cold-formed CHS stub columns.
- Eq. (1) slightly overestimated the strength of CFDST stub columns while Eq. (3) underestimated the strength of CFDST stub columns. Eqs. (2) and (4) gave reasonable predicted strength.
- The predicted ultimate strength of CFDST stub columns using the proposed formula (Eq. (5)) has been found in good agreement with experimental values.
- Increased ductility and energy absorption have been observed for CFDST subjected to compres-

(a) CFDST versus Outer Tube

(b) CFDST versus Outer + Inner Tubes
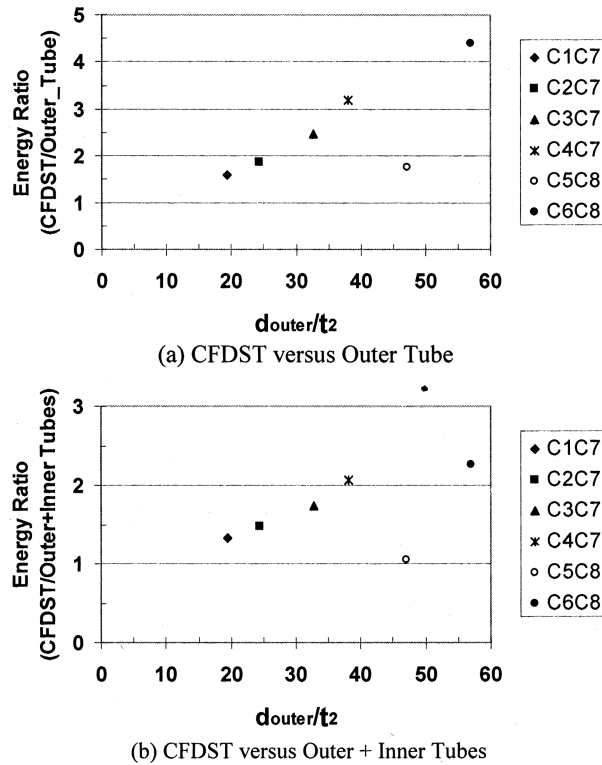
Fig. 12 Energy ratio versus d_{outer}/t

sion especially for slender outer tubes. This emphasizes the efficiency of void-filling for thin sections where often local buckling has detrimental effect on their use as structural members.

Acknowledgements

References

ACI (1995), Building Code Requirements for Reinforced Concrete (ACI, 318-95), and Commentary, American Concrete Institute, Detroit, Michigan, USA.
AISC-LRFD (1999), Load and Resistance Factor Design Specification for Structural Steel Buildings, American Institute of Steel Construction, Chicago, USA.
EC4 (1992), Design of Composite Steel and Concrete Structures, Part 1.1, General Rules and Rules for

Buildings, Eurocode 4, ENV 1994 1-1, 1992.

Elchalakani, M., Zhao, X.L. and Grzebieta, R.H. (2002a), "Plastic mechanism analysis of circular tubes under pure bending", *Int. J. Mech. Sci.*, (accepted for publication).

Elchalakani, M., Zhao, X.L. and Grzebieta, R.H. (2002b), "Plate slenderness Limits for concrete-filled tubes under pure bending", *J. Constr. Steel Res.*, **57**(11), 1141-168.

Elchalakani, E., Zhao, X.L. and Grzebieta, R.H. (2002c), "Tests on concrete filled double skin (CHS Outer and SHS Inner) composite short columns under axial compression, *Thin-Walled Structures,* (accepted for publication).

Grzebieta, R.H. (1990), "On the equilibrium approach for predicting the crush response of thin-walled mild steel structures, *PhD Thesis*, Monash University, Australia.

Kato, B. (1996), "Column curves for steel-concrete composite members", *J. Constr. Steel Res.*, **39**(2), 121-135

Lin, M.L. and Tsai, K.C. (2001), "Behaviour of double-skinned composite steel tubular columns subjected to combined axial and flexural loads", *First Int. Conf. on Steel and Composite Structures*, Pusan, Korea, 1145-1152.

Montague, P. (1978), "The experimental behaviour of double skinned, composite, circular cylindrical shells under external pressure", *J. Mech. Eng. Sci.,* **20**(1), 21-34.

SAA (1991a), Structural Steel Hollow Sections, *Australian Standard AS1163*, Sydney.

SAA (1991b), Methods for Tensile Testing of Metals, *Australian Standard AS1391*, Sydney.

SAA (1994), Concrete Structures, *Australian Standard AS3600*, Sydney.

SAA (1996), Cold-Formed Steel Structures, *Australian/New Zealand Standard AS/NZS4600*, Sydney.

SAA (1998), Seel Structures, *Australian/New Zealand Standard AS/NZS4100*, Sydney.

Shakir-Khalil, H. (1991), "Composite columns of double-skinned shells", *J. Constr. Steel Res.*, **19**, 133-152.

Sugimoto, M., Yokota, S., Sonoda, K. and Yagishita, F. (1997), "A basic consideration on double skin tube-concrete composite columns", Osaka City University and Monash University *Joints Seminar on Composite Tubular Structures*, Osaka City University, Osaka, July.

Tomlinson, M, Chapman, M., Wright, H.D., Tomlinson, A. and Jefferson, A. (1989), "Shell composite construction for shallow draft immersed tube tunnels", *ICE Int. Conf. on Immersed Tube Tunnel Techniques*, April, Manchester, UK.

Wei, S., Mau, S.T., Vipulanadan, C. and Mantrala, S.K. (1995), "Performance of new sandwich tube under axial loading: experimental", *J. Struct. Eng.,* ASCE, **121**(12), 1806-1814.

Wright, H., Oduyemi, T. and Evans, H.R. (1991a), "The experimental behaviour of double skin composite elements", *J. Constr. Steel Res.*, **19**, 91-110.

Wright, H., Oduyemi, T. and Evans, H.R. (1991b), "The design of double skin composite elements", *J. Const. Steel Res.*, **19**, 111-132.

Yagishita, F., Kitoh, H., Sugimoto, M., Tanihira, T. and Sonoda, K. (2000), "Double skin composite tubular columns subjected to cyclic horizontal force and constant axial force", *Proc. the 6th ASCCS Conference,* Los Angeles, USA, 22-24 March, 497-503.

Zhao, X.L. and Grzebieta, R.H. (1999), "Void-filled SHS beams subjected to large deformation cyclic bending", *J. Struct. Eng.*, ASCE, **125**(9), 1020-1027.

Zhao, X.L. and Grzebieta, R.H. (2002), "Strength and ductility of concrete filled double skin (SHS inner and SHS outer) Tubes", *Thin-Walled Structures,* **40**(2), 199-213.

Zhao, X.L., Grzebieta, R.H., Wong, P. and Lee, C. (1999), "Void-filled RHS sections subjected to cyclic axial tension and compression", *Advances in Steel Structures*, S.L. Chan and J. G. Teng (eds), Elsevier, Oxford, 429-436.

Zhao, X.L., Grzebieta, R.H. and Lee, C. (2002), "Void-filled cold-formed rhs braces subjected to large deformation cyclic axial loading", *J. Struct. Eng.*, ASCE, (accepted for publication).
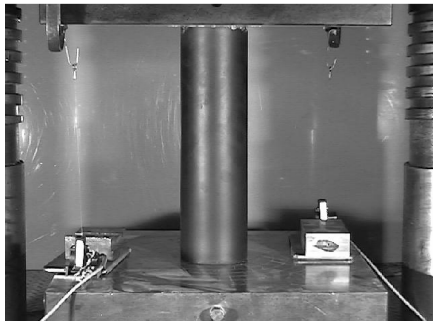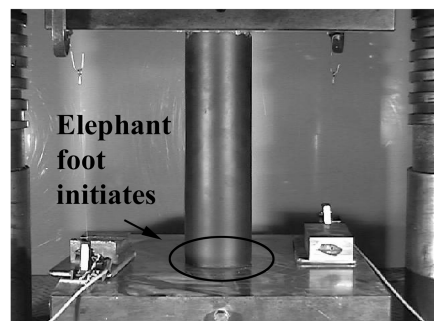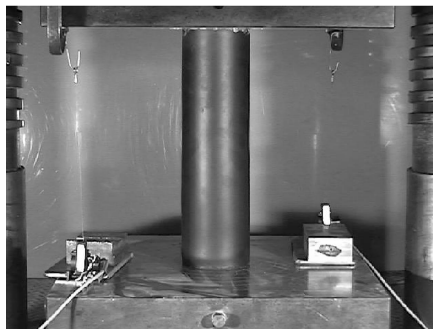
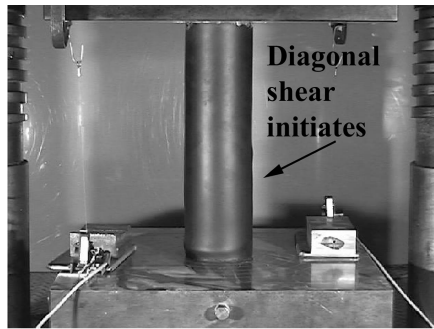## Appendix
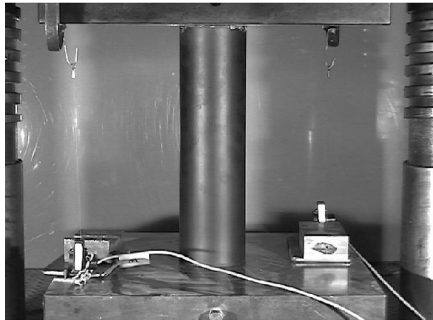
(a) 0 minute
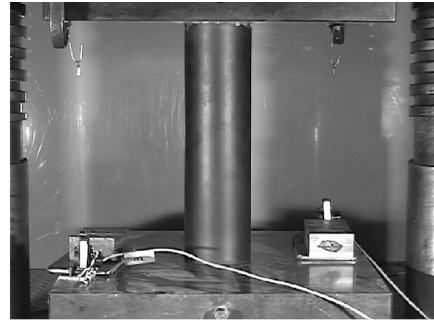
(b) 10 minutes

(c) 15 minutes

(d) 20 minutes

Elephant foot initiates
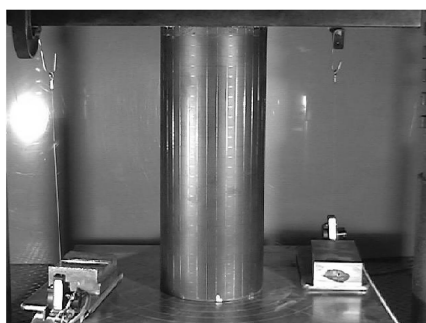
(e) 25 minutes
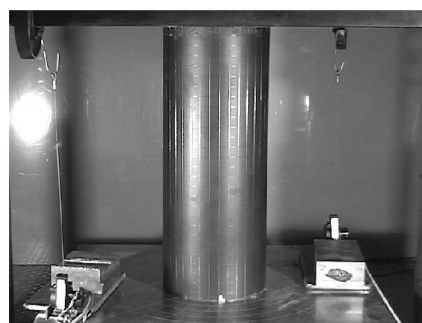
(f) 30 minutes

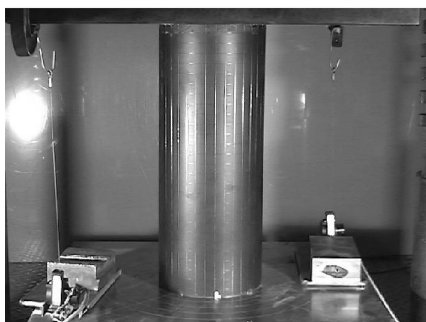**Diagonal shear initiates**
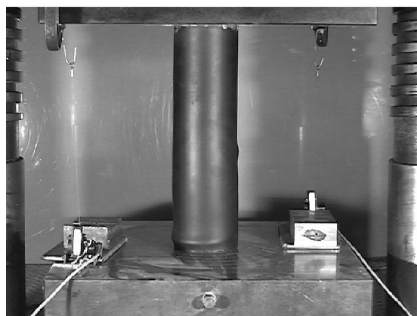
(g) 35 minutes
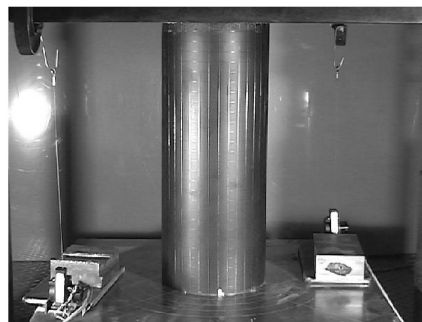
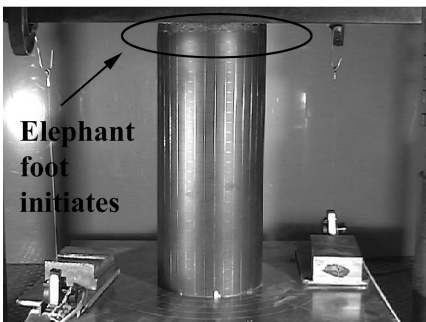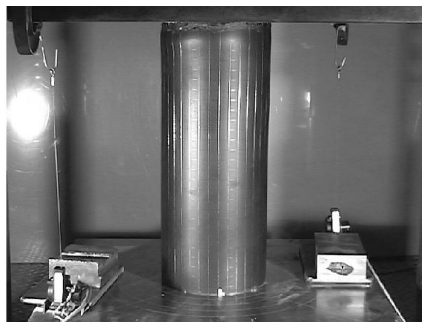**Appendix 1.** Development of failure mode for C4C7

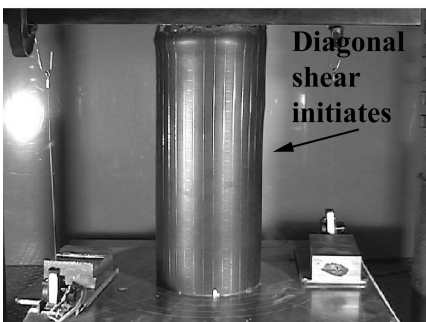(a) 0 minute

(b) 4 minutes

(c) 8 minutes

(d) 12 minutes

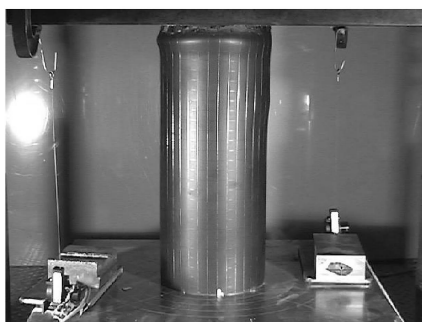**Elephant foot initiates**

(e) 16 minutes

(f) 20 minutes
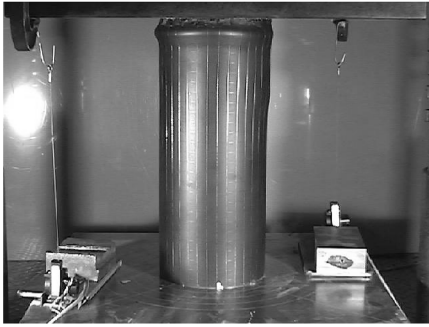
Diagonal shear initiates
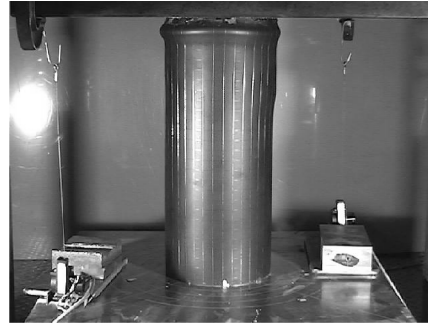
(g) 24 minutes

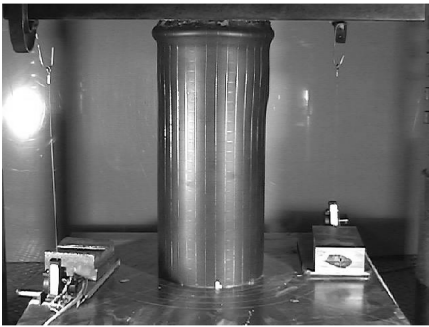(h) 28 minutes

Appendix 2. Development of failure mode for C5C8

(i) 32 minutes   (j) 36 minutes

(k) 40 minutes   (l) 44 minutes
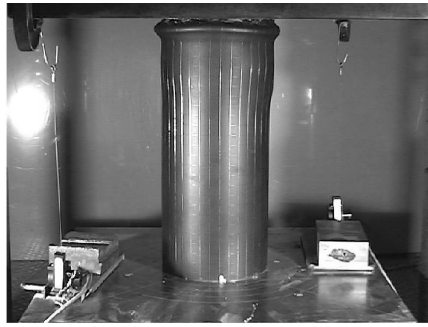
(m) 48 minutes   (n) 52 minutes

Appendix 2. Continued

Notation

A_c	= area of concrete
$A_{innerCHS}$	= cross-section area of the inner CHS
$A_{outerCHS}$	= cross-section area of the outer CHS
D	= diameter of a CHS
d_{inner}	= outside diameter of the inner CHS
d_{outer}	= outside diameter of the outer CHS
d_c	= inner diameter of the outer CHS

E	= Young's modulus of steel tubes
L	= length of a stub column
P_u	= experimental ultimate load for an empty CHS stub column
P_{yn}	= predicted ultimate load for empty CHS based on the nominal yield stress
P_{yt}	= predicted ultimate load for empty CHS based on the measured yield stress
P_{test}	= experimental ultimate load for a CFDST CHS stub column
P_{EC4}	= predicted ultimate load for a CFDST CHS stub column using Eurocode 4
P_{AISC}	= predicted ultimate load for a CFDST CHS stub column using AISC-LFRD
P_{ACI}	= predicted ultimate load for a CFDST CHS stub column using ACI 318-1995
P_{Kato}	= predicted ultimate load for a CFDST CHS stub column using Kato (1996)
P_{theory}	= predicted ultimate load for a CFDST CHS stub column using Eq. (5)
$P_{concrete}$	= predicted load carrying component for concrete
P_{outer}	= predicted load carrying component for the outer CHS
P_{inner}	= predicted load carrying component for the inner CHS
t	= thickness of a CHS
t_1	= thickness of the inner SHS
t_2	= thickness of the outer SHS
t_c	= thickness of the concrete
λ_e	= section slenderness
λ_{ey}	= section slenderness limit
σ_y	= yield stress of steel tube
CK	